JHEP PROCEEDINGS

Heavy Flavours 8, Southampton, UK, 1999

The B-Physics Potential of LHCb, BTeV, ATLAS and CMS

Neville Harnew

Nuclear and Particle Physics Laboratory, University of Oxford, Oxford OX1 3RH, UK.
Email: N.Harnew1@physics.ox.ac.uk

ABSTRACT: The physics performance of the second generation B-physics experiments, LHCb, BTeV, ATLAS and CMS, is reviewed. The differences in detector philosophies, the CP-reach of the experiments, and the sensitivities to rare B decays are compared.

1. Introduction

Prior to 2005, the first generation experiments to study CP-violation in the B system, BaBar, Belle, HERA-B, CDF and D0, will explore the parameters of the unitarity triangle. These parameters, indicated in figure 1, will be determined with varying amounts of precision :

- The quantity $\sin(2\beta)$ will be well measured in the "gold plated" $B^0_d \to J/\psi K_s$ channel, perhaps to $\sim$0.03–0.05;
- The side opposite the angle γ will be known, assuming B^0_s $\overline{B}^0_s$ mixing is measured by CDF and D0;
- The side opposite β will be measured from $b \to u$ decays, but with significant error due to theoretical uncertainty in hadronic interactions;
- The quantity $\sin2(\beta+\gamma)$, i.e. $\sin(2\alpha)$, will be measured, but with poor statistical precision and significant theoretical uncertainty;
- There will be no good or direct measurement of the angle γ. The B_s sector will be largely unexplored by the first generation experiments.

The first generation experiments will either be consistent with the Standard Model interpretation, or will measure inconsistency between the value of β and less precise data, namely the measurement of α and the sides of the triangle. The second generation experiments – LHCb, ATLAS and CMS at the LHC, and BTeV at the Tevatron – will make precision measurements of the same parameters. The high statistics recorded by these experiments will allow the same param-

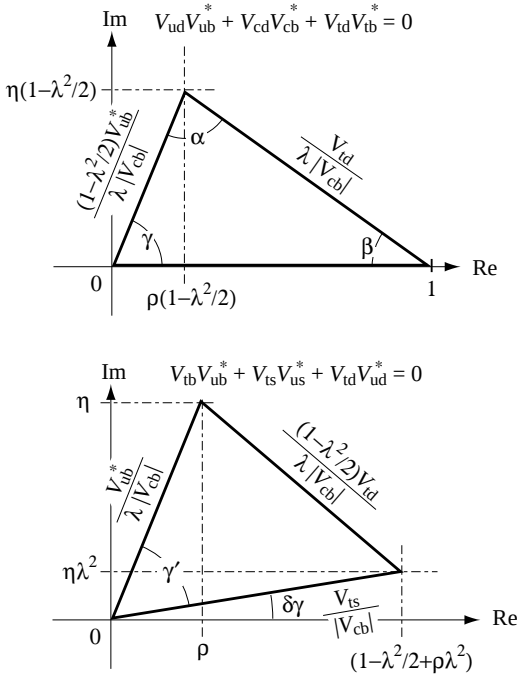

Figure 1: Two unitarity triangles shown in the complex plane, with an approximation valid up to and including $\mathcal{O}(\lambda^5)$. V_{ij} are the CKM matrix elements, and λ is the sine of the Cabibbo angle.

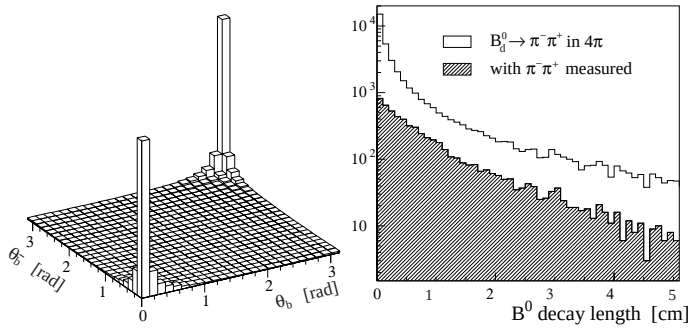

Figure 2: a) The correlation of polar angles of b and $\overline{b}$ hadrons at LHC energies, and b) the corresponding B^0 decay length distribution.

eters to be measured in different channels (which may be theoretically clean but not necessarily the easiest experimentally), giving additional cross checks. New parameters will also be measured with precision in a number of complementary channels, e.g. the angle γ. Experimental attributes of the second generation experiments include efficient π/K identification, excellent decay time resolution, and photon detection.

2. The second generation B physics experiments

A comparison of the LHC and the Tevatron second generation CP violation experiments is given in table 1. The Tevatron (Run II) will collide protons with antiprotons at 2.0 TeV, at which energy the $b\overline{b}$ and inelastic cross sections are expected to be $\sim$100 μb and 50 mb, respectively [1]. The LHC will collide protons with protons at 14.0 TeV. The increased energy gives a $b\overline{b}$ cross section $\sim$5 times higher than the Tevatron, and with an inelastic cross section which is only a factor of 1.6 higher, 80 mb. Both LHCb and BTeV experiments have forward geometries whereas ATLAS and CMS are general-purpose detectors, covering the central rapidity region.

There are a number of advantages associated with forward detector geometry. The first advantage is the increased B acceptance; the $b\overline{b}$ production cross section is sharply peaked in the forward-backward direction. This is demonstrated in figure 2a which shows the correlation of the polar angles of b and $\overline{b}$ hadrons, defined with respect to the beam in the pp centre of mass system, at LHC energies. The second advantage of forward geometry is that a vertex detector can be placed close to the interaction region. At the LHC, the mean momentum for accepted B mesons is $\sim$80 GeV/c, leading to a mean B^0 decay length of $\sim$7 mm, shown in figure 2b. Excellent proper time resolutions of approximately 40–50 fs can be achieved. Finally, the open geometry allows for easy installation and maintenance of the detector components.

One disadvantage of the forward geometry is that minimum bias events are also strongly forward peaked. This gives high track densities which result in high particle occupancies.

2.1 The LHCb Experiment

The LHCb detector [2] is a forward single-arm spectrometer, shown in figure 3. LHCb has a precision silicon strip vertex detector for measurement of B decay vertices, giving a 120 μm resolution along the z axis. Here radial and azimuthal cordinates with respect to the beam axis are measured with r and ϕ strips, respectively. A dipole magnet provides a field integral (B.dL) of 4 Tm. There is an efficient four level trigger system (designated Level-0 to Level-3), with a vertex trigger included at Level-1. Two RICH detectors, shown in figure 4, provide particle identification with at least a 3σ π/K momentum separation between $1 < p < 150$ GeV/c. The upstream detector, RICH-1, uses C_4F_{10} gas (giving π and K thresholds of 2.6 and 9.3 GeV/c, respectively) and aerogel (giving thresholds of 0.6 and 2.0 GeV/c, respectively). The downstream detector, RICH-2, uses CF_4 gas (giving π and K

	Tevatron	LHC	
Energy / collision mode	2 TeV $p\overline{p}$	14 TeV pp	
$b\overline{b}$ cross section	$\sim$100 μb	$\sim$500 μb	
Inelastic cross section	50 mb	80 mb	
Ratio $b\,\overline{b}$ / inelastic	0.2%	0.6%	
Bunch spacing	132 ns	25 ns	
	BTeV	LHCb	ATLAS / CMS
Detector configuration	Two-arm forward	Single-arm forward	Central detector
Running luminosity	2×10^{32}cm^{-2}s^{-1}	2×10^{32}cm^{-2}s^{-1}	$\leq1\times10^{33}$cm^{-2}s^{-1}
$b\,\overline{b}$ events per 10^7 sec	$2\times10^{11}\times$ accept.	$1\times10^{12}\times$ accept.	$\leq5\times10^{12}\times$ accept.
<Interactions/crossings>	$\sim$2.0	0.5 ($\sim$30% single int.)	$\sim$2.3

Table 1: Comparison of the LHC and the Tevatron experiments.

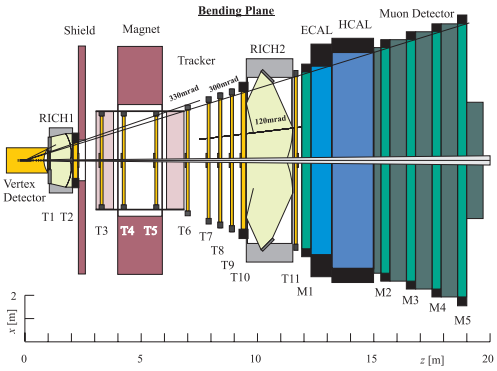

Figure 3: A schematic of the LHCb detector.

thresholds of 4.4 and 15.6 GeV/c, respectively). Hadron and electromagnetic calorimetry is employed, primarily to trigger on hadrons, electrons and photons.

The high B event rate means that running LHCb at low luminosity is sufficient when operating with a highly efficient trigger, discussed below. By de-tuning the beam focus, LHCb will run at a luminosity of 2.0×10^{32} cm^{-2}s^{-1}. This gives an average of only $\sim$0.5 interactions per bunch crossing. Having a single primary vertex has distinct advantages in reducing confusion to the trigger, reducing particle occupancy, and hence improved pattern recognition in the detector components. Low luminosity also ensures less radiation damage.

The Level-0 trigger of LHCb comprises a muon, electron and hadron trigger, which pre-selects high p_T (>1–2 GeV/c) tracks and clusters. A "pile-up" veto trigger ensures that >80% of events will contain only one single beam interaction. The Level-1 vertex trigger then selects detached vertices in software. This has excellent efficiency for B decays of interest : 50%, 48% and 56% for $B^0 \to J/\psi K^0_s(\mu\mu)$, $B^0 \to \pi^+\pi^-$ and $B^0_s \to D^-_s K^+$, respectively. Level-2 and Level-3 are software triggers which refine the p_T and vertex requirements, and select B decay channels of interest. The combined efficiency of all trigger levels is typically 30% for reconstructable events within the spectrometer. These trigger efficiencies are "diluted" by tagging efficiencies which are typically 40%, and by wrong tag fractions which are typically 30%.

The importance of the LHCb RICH detectors in providing particle identification is demonstrated in figure 5. This shows the effect of reducing background in the channel $B_d \to \pi^+\pi^-$ (which has a visible branching ratio $< 0.7\times10^{-5}$). Without utilizing RICH information, the $\pi^+\pi^-$ mass distribution suffers serious background from the channels $B_d \to K^\pm\pi^\mp$ (BR. 1.5×10^{-5}), $B_s \to K^+K^-$ (BR. 1.5×10^{-5}), and $B_s \to K^\pm\pi^\mp$ (BR. 0.7×10^{-5}). These channels can themselves demonstrate CP asymmetries and, if not rejected, can dominate the $B_d \to \pi^+\pi^-$ asymmetry. It can be seen that the effect of the π/K identification provided by the RICH detectors offers almost complete background rejection, with an 85% efficiency. The excellent mass resolution in this channel, 17 MeV, also greatly aids background suppression.

2.2 The BTeV Experiment

The BTeV detector [3] is a forward-backward double arm spectrometer, shown in figure 6. The

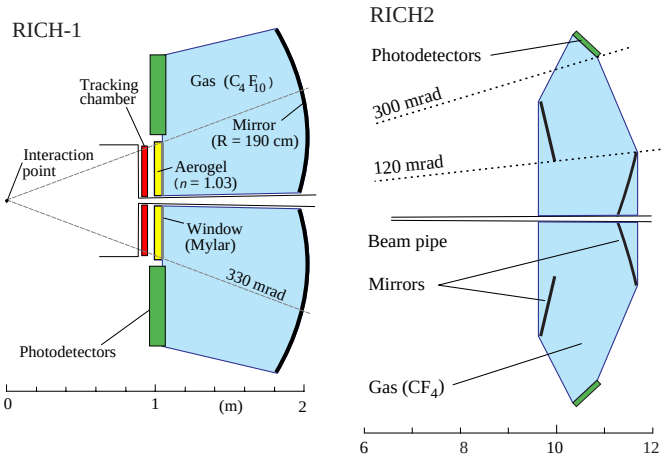

Figure 4: Schematics of the LHCb RICH-1 and RICH-2 detectors.

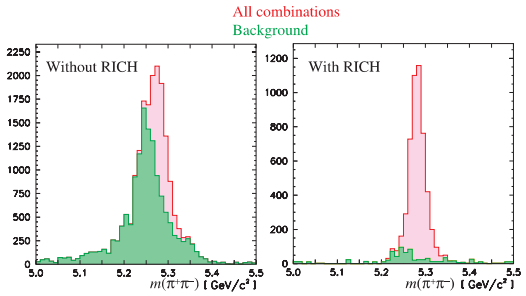

Figure 5: B_s^0 mass peak from $\pi^+\pi^-$ combinations in LHCb, showing the background from channels described in the text, without and with RICH information.

double arm gives BTeV a relative rate advantage of ∼2 with respect to LHCb. A precision pixel vertex detector is sited inside a dipole magnet of field integral 5.2 Tm. BTeV utilizes a RICH detector which provides particle identification between 3 and 70 GeV/c (the momentum spectrum is softer than at the LHC). A lead tungstate EM calorimeter allows reconstruction of photons and π^0's with high resolution.

The key design feature of BTeV is the utilization of a pixel vertex detector, shown in figure 7. This detector provides excellent spatial resolution of 5–10 μm, giving a B proper time resolution of ∼50 ps. The pixels have good signal to noise, they ensure low particle occupancy, and the detectors are intrinsically radiation hard. The special feature is an ambitious vertex trigger at the first level, which selects generic B meson decays, keeping biases to a minimum. The location of the pixel detector in the B field also facilitates background rejection at the trigger level from low momentum tracks and secondary interactions. The disadvantage of the pixel detector is that it has excessive material thickness, a total of ∼1 radiation lengths, although typical tracks traverse only a fraction of this. BTeV will run at the full luminosity of the Tevatron, 2.0×10^{32} cm^{-2}s^{-1}, giving an average of ∼2 interactions per bunch crossing

BTeV has a three level trigger system. Level-1 is the vertex trigger which is pipelined at 132 ns. The vertex trigger has excellent efficiency for B decays of interest : 50%, 55% and 70% for $B^0 \to J/\psi K_s^0(\mu\mu)$, $B^0 \to \pi^+\pi^-$ and $B_s^0 \to D_s^- K^+$, respectively. The Level-2 and Level-3 triggers are software triggers, which select B decays of interest. Tagging efficiencies and wrong tag fractions are similar to LHCb.

2.3 The ATLAS/CMS Experiments

ATLAS and CMS [4, 5] are the two LHC general-purpose detectors. Both detectors have tracking coverage in the central rapidity region, $|\eta|$ <2.5. The detectors have specialist B triggers which can operate up to luminosities of typically 1×10^{33} cm^{-2}s^{-1}. The detectors have no dedicated hadronic particle identification capabilities (with the exception of a limited dE/dx measurement in ATLAS).

ATLAS and CMS incorporate three levels of

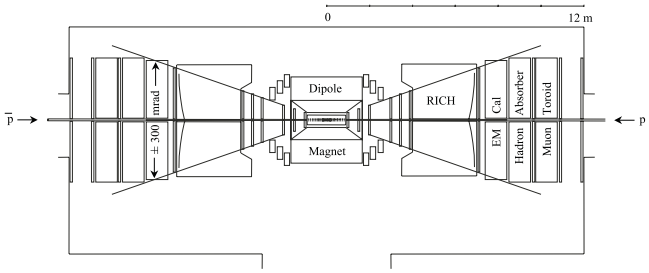

Figure 6: A schematic of the BTeV detector.

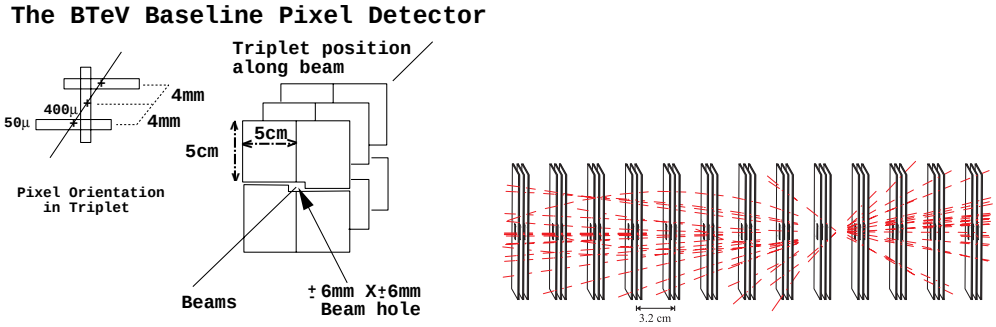

Figure 7: A schematic of the BTeV pixel detector showing a) the layout, and b) a simulated $B^0 \to \pi^+\pi^-$ event.

trigger. High p_T (5-6 GeV/c) muon and calorimeter triggers are incorporated at Level-1. Level-2 and 3 are software triggers which, for low and modest luminosity running, allow selection of B's with high statistics. Neither experiment incorporates a dedicated vertex trigger at an early level.

3. B physics capabilities

The CP physics reach of the second generation experiments in specific benchmark channels for a year of operation, together with the triangle parameters which they measure, is summarised in table 2. A selection of important measurements is described below.

3.1 Measurement of the angle β via $B_d \to J/\psi K^0_s$

The channel $B_d \to J/\psi K^0_s$ provides a "gold-plated" measurement of $\sin(2\beta)$. The decay asymmetry :

$$A(t) = \frac{B_d \to J/\psi K^0_s - \overline{B}_d \to J/\psi K^0_s}{B_d \to J/\psi K^0_s + \overline{B}_d \to J/\psi K^0_s} = -\sin(2\beta)\sin(\Delta m t),$$

where Δm is the mass difference of the two weak eigenstates of the $B_d - \overline{B}_d$ system, is largely insensitive to the contribution from penguin amplitudes. Here the sensitivities of the general-purpose detectors compete well with those of the forward detectors, due to the formers' efficient high p_T muon triggers [4, 5]. The invariant mass distribution of $J/\psi K^0_s$ combinations, together with the estimated background, is shown for ATLAS in figure 8. Table 2 demonstrates that $\sin(2\beta)$ can be measured to an accuracy of 0.02 or better in this channel by each of the second generation experiments in a year of operation.

3.2 Measurement of the angle γ

3.2.1 $B^0_s \to D^-_s K^+$

The channel $B^0_s \to D^-_s K^+$ and its charge conjugate states provide a measurement of the angle $(\gamma - 2\delta\gamma)$ [7]. Four time-dependent decay rates are measured : $B^0_s \to D^-_s K^+$, $B^0_s \to D^+_s K^-$, $\overline{B}^0_s \to D^-_s K^+$ and $\overline{B}^0_s \to D^+_s K^-$, which yield values for $(\gamma - 2\delta\gamma)$ and the strong phase difference, Δ. The importance of particle identification and good mass resolution is demonstrated for LHCb in figure 9. In the absence of particle

Measurement	Channel	LHCb	BTeV	ATLAS	CMS
$\sin(2\beta)$	$B_d^0 \to J/\psi K_s^0$	0.011 – 0.017	0.021	0.021	0.025
$\sin(2\alpha)$	$B_d^0 \to \pi^+\pi^-$	0.05	0.06	0.10	0.17
$\sin(2\alpha)$, $\cos(2\alpha)$	$B_d^0 \to \rho\pi$	$\sigma(\alpha) \sim 5°$		–	–
$2\beta + \gamma$	$B_d^0 \to D^\star\pi$, 3π	9°		–	–
$\gamma - 2\delta\gamma$	$B_s^0 \to D_s^- K^+$	6 – 13°	11°	–	–
γ	$B_d^0 \to D^0 K^{\star 0}$	10°		–	–
γ	$B^- \to D^0 K^-$		13°	–	–
$\delta\gamma$	$B_s^0 \to J/\psi\phi$	0.6°		0.9°	
x_s	$B_s^0 \to D_s^-\pi^+$	< 75	< 60	< 46	< 48
Rare decay	$B_s^0 \to \mu^+\mu^-$	4.4σ S.M.		4.3σ S.M.	10σ S.M.
Rare decay	$B_d^0 \to K^{\star 0}\gamma$	26k events	24k events	–	–

Table 2: Performance summary of the second generation experiments in a selection of benchmark channels for one year of operation. The quoted numbers are the errors on the parameter in question, unless specified otherwise. The α measurement in the $B_d^0 \to \pi^+\pi^-$ channel assumes no penguin contribution. The $B_s^0 \to \mu^+\mu^-$ channel assumes a Standard Model branching ratio of 3.5×10^{-9}. A dash for an entry means that no significant measurement can be made. If an entry is left blank, this means that a measurement of significance is expected, but still needs to be fully studied.

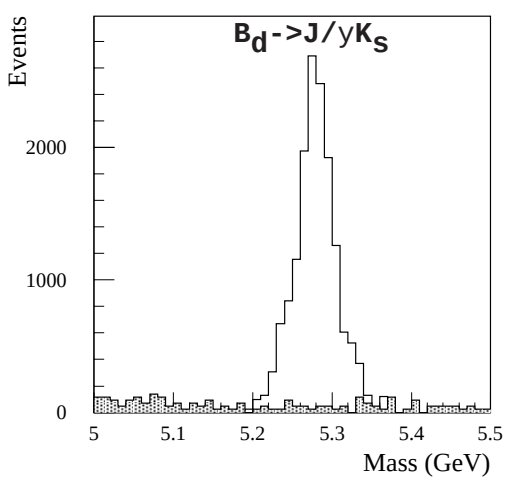

Figure 8: Invariant mass distribution of J/ψ combinations with the background estimate superimposed (shaded histogram).

identification, the signal is dominated by background from $B_s^0 \to D_s^-\pi^+$ decays (the B_s mixing channel).

Sensitivities per year to $(\gamma - 2\delta\gamma)$ depend on $(\gamma - 2\delta\gamma)$, and on Δ. An example of a fit to 1000 Monte Carlo BTeV "experiments" is shown

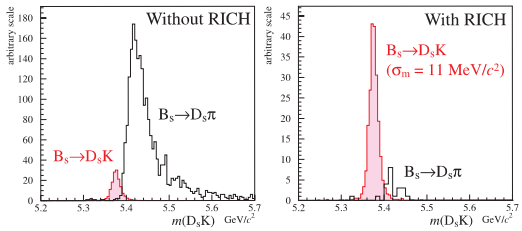

Figure 9: B_s^0 mass peak from D_sK combinations in LHCb, showing the background from $D_s\pi$, with and without RICH information.

in figure 10. Table 2 demonstrates that BTeV and LHCb can achieve sensitivities of 6–13° in $(\gamma - 2\delta\gamma)$ for one year of running.

3.2.2 $B_d^0 \to D^0 K^{\star 0}$

The channel $B_d^0 \to D^0 K^{\star 0}$ and its charge conjugate states provide a measurement of the angle γ. Six time-integrated decay rates are measured : $B_d^0 \to D^0 K^{\star 0}$, $B_d^0 \to \overline{D}^0 K^{\star 0}$, $B_d^0 \to D^0_{CP=+1} K^{\star 0}$, $\overline{B}_d^0 \to \overline{D}^0 \overline{K}^{\star 0}$, $\overline{B}_d^0 \to D^0 \overline{K}^{\star 0}$ and $\overline{B}_d^0 \to D^0_{CP=+1} \overline{K}^{\star 0}$. $D^0_{CP=+1}$ signifies the decay of the D^0 into a CP eigenstate, i.e. K^+K^- or $\pi^+\pi^-$, otherwise $D^0 \to K^+\pi^-$ decays are considered. Since visible branching ratios are very small $(10^{-8} - 10^{-7})$, the measurements are only possible with a high-rate for-

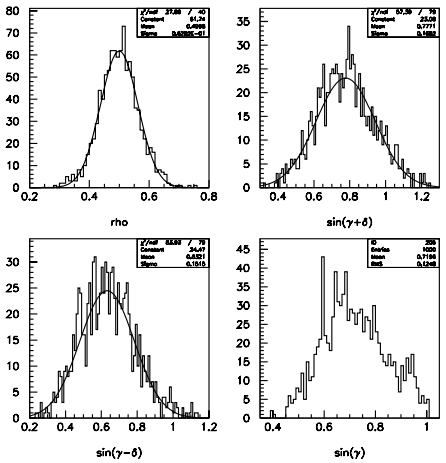

Figure 10: Example of fitting γ in the channel $B_s^0 \to D_s^- K^+$ for 1000 BTeV Monte Carlo "experiments". The values γ=45°, $\sin(\gamma + \Delta)$=0.771, $\sin(\gamma - \Delta)$=0.629 and ρ=0.5 are assumed, yielding a fitted value of γ of 46^{+11}_{-9} degrees.

ward detector utilizing particle identification (i.e. LHCb and BTeV).

LHCb have evaluated the sensitivity of the γ measurement in these channels. The B_d^0 reconstructed in the $B_d^0 \to \overline{D}^0 K^{\star 0}$ channel is shown in figure 11, demonstrating the importance of particle identification. Using this method, LHCb can measure the angle γ to a precision of $\sim$10° after one year of running.

3.2.3 $B^- \to D^0 K^-$

The channel $B^- \to D^0 K^-$ provides a measurement of the angle γ via nine time-integrated decay rates [3, 8]. CP-violation arises from the interference between the decays $B^- \to D^0 K^-$ and $B^- \to \overline{D}^0 K^-$, where the D^0 and $\overline{D}^0$ decay into the same final state (similarly for the charge conjugate decays). It is necessary to measure the branching ratios BR($B^- \to f_i K^-$) for the D^0 and $\overline{D}^0$ decaying into at least two different final states f_i in order to determine γ up to discrete ambiguities. Using this method, BTeV can measure the angle γ to a precision of $\sim$13° after one year of running. The decay modes $D^0, \overline{D}^0 \to K^+\pi^-$ and K^+K^- have been studied.

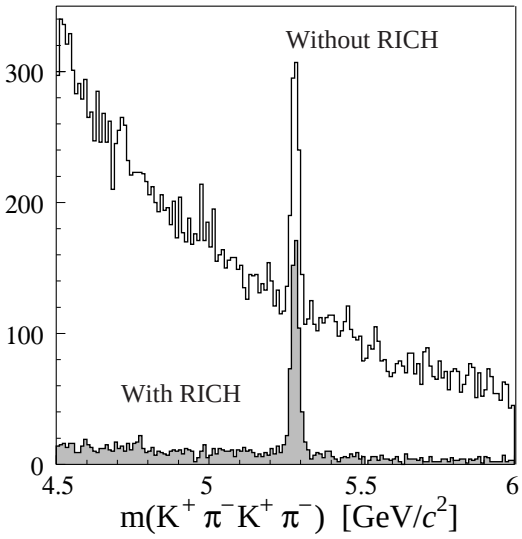

Figure 11: B_d^0 mass peak from $K^+\pi^-K^+\pi^-$ combinations in LHCb, with and without RICH information.

3.2.4 $B_d^0 \to D^\star\pi$ and $D^\star 3\pi$

The channels $B_d^0 \to D^{\star\pm}\pi^\mp$ and $D^\star 3\pi$ provide measurements of the angle $(2\beta+\gamma)$ via four time-dependent decay rates [2, 9]. Small CP asymmetries, $\sim$1%, result from the interference of the tree diagram with the doubly-Cabibbo suppressed decay into the same final state. LHCb have studied the sensitivity of these channels in which large statistics are vital, and so are reliant on an efficient hadron trigger. The method involves an inclusive $D^\star$ reconstruction technique, yielding 270 k events per year in the channel $B_d^0 \to D^{\star\pm}\pi^\mp$, with a signal to background of $\sim$7. Including the $D^\star a_1$ ($a_1 \to 3\pi$) channel gives an additional 320 k events/year.

The error on $(2\beta+\gamma)$ is shown as a function of $(2\beta+\gamma)$ in figure 12, assuming no strong phase difference. The angle γ can be measured to a precision of 5° after five years of running.

3.3 Measurement of the angle α via $B_d^0 \to \rho\pi$

The analysis of B_d^0 decays to three pions leads to an alternative determination of the angle α. This complements the $B_d^0 \to \pi^+\pi^-$ measurement, which has large penguin uncertainties. The interesting decays have ρ mesons in the intermediate state : $B_d^0 \to \rho^+\pi^-$, $B_d^0 \to \rho^-\pi^+$ and $B_d^0 \to$

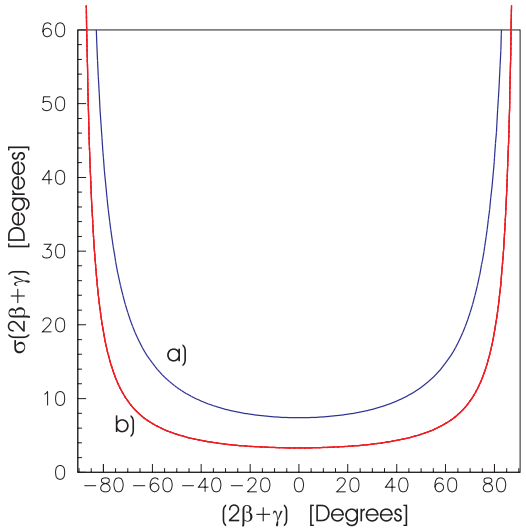

Figure 12: The error on $(2\beta + \gamma)$ as a function of $(2\beta + \gamma)$ after a) one and b) five years of LHCb running.

$\rho^0\pi^0$. A time-dependent analysis of the Dalitz plot allows the extraction of α, as well as the tree and penguin terms separately. The interference between the ρ^+, ρ^- and ρ^0 amplitudes, occuring at the intersection of the Dalitz plot bands, allows the determination of $\cos 2\alpha$ and $\sin 2\alpha$. This removes ambiguities in the determination of α.

The LHCb and BTeV collaborations have performed simulation studies of the $B^0_d \to \pi^+\pi^-\pi^0$ final state. BTeV has lead tungstate electromagnetic calorimetry which provides excellent energy resolution ($\sim 2\%/\sqrt{E} \oplus 0.6\%$) and fine granularity for photon detection and π^0 reconstruction. LHCb utilizes coarser granularity Shashlik electromagnetic calorimetry ($\sim 10\%/\sqrt{E} \oplus 1.5\%$), but has a large 12 m lever arm for separation of the gammas. BTeV expect ~3000 fully tagged $\rho^+\pi^-$ events per year [3], and although a complete GEANT simulation and background rejection study still needs to be performed, the high resolution calorimetry should give the experiment a clear advantage. LHCb have performed a detailed study [2], and expect annual event yields of triggered, fully reconstructed and tagged events to be : $\rho^+\pi^-$ ~ 1000 (BR. = 44×10^{-6}), $\rho^-\pi^+$ ~ 200 (BR. = 10×10^{-6}), and $\rho^0\pi^0$ ~ 50 (BR. = 1×10^{-6}), where the branching ratios used are those theoretically predicted. These rates are to be compared with the $B^0_d \to \pi^+\pi^-$ channel, which for LHCb yields ~ 7000 events per year, assuming a branching ratio of 7×10^{-6}.

Figure 13a shows the expected $\pi^+\pi^-\pi^0$ invariant mass distribution after one year of LHCb data taking. The measured B^0_d width is 50 MeV/c^2 and the expected signal to background is ~0.75. Figure 13b shows the expected signal distribution in this channel for BTeV.

In principle, a nine parameter fit can be performed to the time-dependent Dalitz plot, yielding α and the tree and penguin amplitudes. Preliminary studies from LHCb indicate that an accuracy in α of ~5% could be reached after one year of data taking.

3.4 Measurement of x_s via $B^0_s \to D^-_s\pi^+$

$B_s - \overline{B}_s$ oscillations have been studied in the channels $B^0_s \to D^-_s\pi^+$ and $\overline{B}^0_s \to D^+_s\pi^-$, and all second generation experiments can make measurements of x_s beyond Standard Model expectations. A simulation of $B_s - \overline{B}_s$ oscillations in BTeV, together with a fit to x_s, is shown in figure 14. A similar simulation for LHCb is shown in figure 15. Table 2 demonstrates that x_s will be measured to 45 or better by each of the second generation experiments in a year of operation.

3.5 The $B^0_s \to \mu^+\mu^-$ rare decay

The $B^0_s \to \mu^+\mu^-$ channel is an example of a Standard Model rare decay process, with an expected branching ratio of $\sim 3.5\times10^{-9}$ [10]. Here the high p_T di-muon triggers running at high luminosity (1×10^{34} cm^{-2}s^{-1}) give the general-purpose detectors a distinct advantage over the forward detectors to observe this channel. CMS have excellent muon detection capabilities [5]. They expect 26 signal events with 6.4 events background for 100 fb^{-1} of running (i.e. 10^7s at 1×10^{34} cm^{-2}s^{-1}) [11]. The expected CMS di-muon effective mass distribution for the B^0_s decay is shown in figure 16, yielding a resolution of 31 MeV.

4. Summary

The second generation CP-violation experiments, LHCb, BTeV, ATLAS and CMS, will measure CP violation parameters with huge statistics, $\sim 10^{12}\ b\overline{b}$

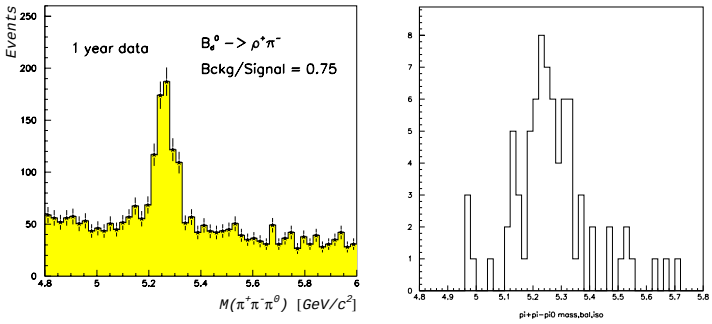

Figure 13: Simulated $\pi^+\pi^-\pi^0$ invariant mass distributions from a) LHCb, showing the B mass peak and expected signal to noise, and b) BTeV, showing the signal only.

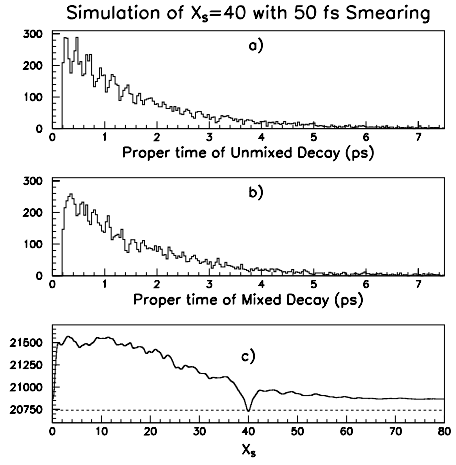

Figure 14: Monte Carlo proper lifetime distributions from BTeV : a) for $B_s^0 \to D_s^-\pi^+$ tagged as B_s^0, b) for $B_s^0 \to D_s^-\pi^+$ tagged as $\overline{B}_s^0$, and c) the negative log-likelihood of the fitted value of x_s as a function of x_s. (Here the simulated x_s value is 40, with a 50 fs time smearing of the B_s decay time).

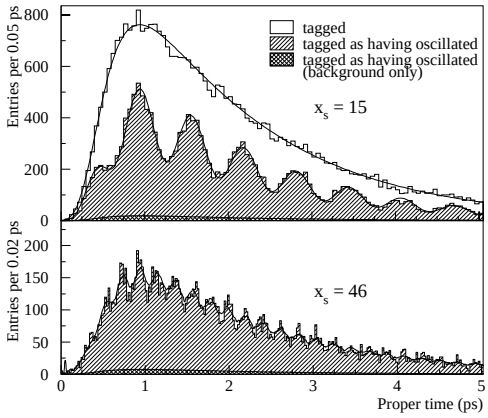

Figure 15: Monte Carlo proper lifetime plots from LHCb of $B_s^0 \to D_s^-\pi^+$ tagged as B_s^0 and $\overline{B}_s^0$, a) for x_s=15, and b) for x_s=46.

pairs per year. The LHCb and BTeV experiments will utilize vertex detectors which will give proper time resolutions of σ_t ∼40–50 fs, and provide efficient B secondary vertex triggers. K/π particle identification will be essential for the measurement of B final states involving hadrons.

The second generation experiments will measure the angles and the sides of the unitarity triangles with unprecedented precision. This will be a unique opportunity to understand the origin of CP violation in the framework of the Standard Model, and beyond.

Acknowledgments

I am very grateful to the following people who provided material for this review : Nick Ellis and Roger Jones (ATLAS), Daniel Denegri and Andrei Starodoumov (CMS), Sheldon Stone (BTeV), and Tatsuya Nakada and Guy Wilkinson (LHCb). I also extend my thanks to the Heavy Flavour 8 organizers, and personally to Paul Dauncey and Jonathan Flynn, for making the conference in Southampton so enjoyable.

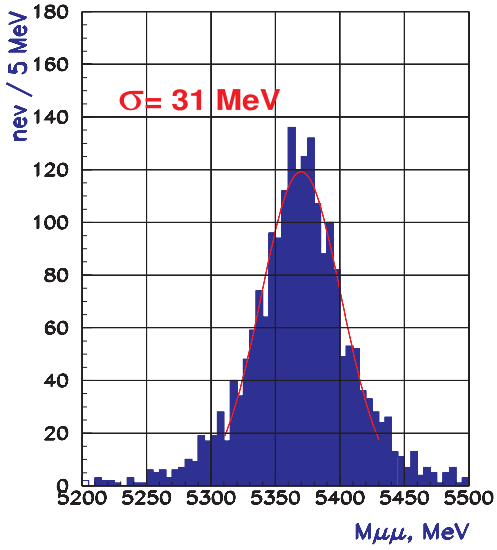

Figure 16: The di-muon effective mass distribution in CMS. Two muons are triggered with p_T >4.3 GeV over the rapidity region $|\eta| < 2.4$.

References

[1] F. Abe et. al., CDF Collaboration, *Phys. Rev.* **D 50** (1994) 5550.
CDF Collaboration, Fermilab/PUB-96/390E.

[2] "A Large Hadron Collider Beauty Experiment for Precision Measurements of CP Violation and Rare Decays"; LHCb Technical Proposal, LHCC 98/04, LHCC/P4 (Feb. 1998).

[3] "Proposal for an Experiment to Measure Mixing, CP Violation and Rare Decays in Charm and Beauty Particle Decays at the Fermilab Collider - BTeV." BTeV Preliminary Technical Design Report (May 1999).
See http://www-btev.fnal.gov/btev.html

[4] "A General-Purpose pp Experiment at the Large Hadron Collider at CERN." ATLAS Technical Proposal. CERN/LHCC/94-43 (December 1994).

[5] "The Compact Muon Solenoid." CMS Technical Proposal CERN/LHCC 94-38 (December 1994).

[6] ATLAS Detector and Physics Performance Technical Design Report. ATLAS Collaboration, Vol I and II, CERN/LHCC/99-14 and 15 (May 1999).

[7] See for example R. Aleksan, I. Dunietz and B. Kayser, *Z. Physik* **C 54** (1992) 653.

[8] M. Gronau and D. Wyler, *Phys. Lett.* **B 265** (1991) 172.
D. Atwood, I.Dunietz and A. Soni, *Phys. Rev. Lett.* **78** (1997) 3257.

[9] I. Dunietz, Beauty'97, *Nucl. Instr. Meth.* **A408** (1998) 14.

[10] A. Ali, Beauty'96, *Nucl. Instr. Meth.* **A384** (1996) 8.

[11] D. Denegri private communication, and A. Starodoumov, Beauty'99, Bled, Slovenia (to be published in *Nucl. Instr. Meth.*).